# Reexamination of measurement-induced chaos in entanglement-purification protocols

Yilun Guan, Duy Quang Nguyen, Jingwei Xu, and Jiangbin Gong
*Department of Physics, National University of Singapore, 117542 Singapore*
(Received 28 February 2013; published 20 May 2013)

Entanglement-purification protocols, developed for the sake of high-fidelity communication through noisy quantum channels, are highly nonlinear quantum operations and can offer a very useful context to studies of nonlinear complex maps. Recently it was demonstrated that the feedback mechanism used in a typical purification protocol can cause the evolution dynamics of qubits to exhibit chaos [Kiss *et al.*, Phys. Rev. Lett. **107**, 100501 (2011)]. In this work we extend the investigation by considering the natural time evolution of qubits during a purification process, leading to a number of interesting findings that reflect the competition between the natural unitary evolution of qubits and nonlinear purification operations. As a result, the overall evolution dynamics of entanglement can be much richer. Possible applications are also proposed.

DOI: 10.1103/PhysRevA.87.052316 PACS number(s): 03.67.Mn, 03.67.Ac, 05.45.Mt, 42.50.Lc

## I. INTRODUCTION

Producing and protecting high-fidelity entanglement is one of the biggest challenges in the context of quantum communication. More often than not it is required that the noise level in the entanglement must be controlled at an acceptable level for successful implementation of various tasks of quantum information transfer. To address the problems of communication along noisy quantum channels many entanglement-purification protocols have been developed. The process of entanglement purification distills a number of maximally entangled states from a larger pool of noisy, nonmaximally entangled states [1]. The purification operations must be nonlinear as they involve measurements. This fact hints that entanglement-purification protocols can offer an intriguing quantum-physics context for nonlinear dynamics studies. In particular an entanglement-purification protocol may be described as nonlinear maps on a complex plane and the associated dynamics has not been studied extensively.

In a few early studies Kiss *et al.* demonstrated that the entanglement of two-qubit systems can evolve chaotically under certain purification protocols [2–4]. More specifically, it was shown that the outcome of long-time iteration of certain purification protocols, e.g., a maximally entangled state or a completely separable state is strongly sensitive to initial states due to the nature of chaos. Other dynamical phenomena presented in Refs. [2–4] are also stimulating. However, the role of the natural time evolution of the qubit systems still has not been accounted for yet. The aim of this work is to investigate how the entanglement dynamics in purification protocols might be affected if we allow the qubit system to evolve during the process of purification. This extension is of interest for at least two reasons. First, based on previous lessons learned from the so-called quantum Zeno effect and quantum anti-Zeno effect [5–8], it is expected that the competition between the natural time evolution of the system and the nonlinear operations such as measurements often yields new understandings of physics and also new means for quantum manipulations. Second, any physical process takes time to complete and by considering a new time parameter characteristic of the natural time evolution of the concerned system (whose states are under purification), we may get one more step closer to the actual purification dynamics. In doing so we are also rewarded with a wider class of nonlinear maps. In particular we demonstrate that the competition between the natural time evolution of a two-qubit system and the speed of the purification process does have a big impact on the overall evolution dynamics of the system. Our detailed results suggest that the interplay between the system's own evolution and nonlinear operations can lead to highly complex quantum dynamics, which goes well beyond the quantum Zeno effect and quantum anti-Zeno effect.

## II. A COMPLEX NONLINEAR QUANTUM MAP ACCOUNTING FOR SYSTEM'S NATURAL EVOLUTION

In this work we focus on a particular entanglement-purification protocol that makes use of a nonlinear transformation (denoted by **S**) followed by a unitary transformation (**U**) as depicted schematically in Fig. 1. The system under purification consists of two qubits. Following the treatment of Kiss *et al.* [2–4], we consider a pure two-qubit state $|\psi\rangle = c_1|00\rangle + c_2|01\rangle + c_3|10\rangle + c_4|11\rangle$. A nonlinear transformation **S** performs the mapping $c_i \xrightarrow{\mathbf{S}} Nc_i^2$, where $N$ is a normalization constant [9]. In the protocol under consideration here, we choose the unitary transformation to be $\mathbf{U} = \mathbf{H} \otimes \mathbf{H}$, where **H** is the one-qubit Hadamard transformation [$H_{ij} = (-1)^{ij}/\sqrt{2}$]. For a restricted class of nonmaximally entangled state $|\psi\rangle = N_1(|00\rangle + \xi|11\rangle)$ ($\xi \in \mathbb{C}$) as initial states, one iteration of the purification process yields $|\psi^{(1)}\rangle = \mathbf{US}|\psi\rangle$. Two successive iterations map the state $|\psi\rangle$ to $|\psi^{(2)}\rangle = N_2(|00\rangle + g(\xi)|11\rangle)$, where $g(\xi) : \mathbb{C} \to \mathbb{C}$ and

$$g(\xi) = \frac{2\xi^2}{1+\xi^4}. \tag{1}$$

It was demonstrated by Kiss *et al.* that, under the map $\xi \to g(\xi)$, the values of $|g(\xi)|$ converge asymptotically to either 0 or 1, corresponding to separable and maximally entangled states, respectively [2]. The final converged state shows strong sensitivity to initial values of $\xi$. To examine possible effects of the natural time evolution of the two qubits, we now consider a modified scheme illustrated in Fig. 2, which is based on the same purification protocol defined by **S** and **U**, but with a $\Delta t$ time lapse between the two successive steps. The system's own time evolution occurs during $\Delta t$. Note that to maintain

 ©2013 American Physical Society

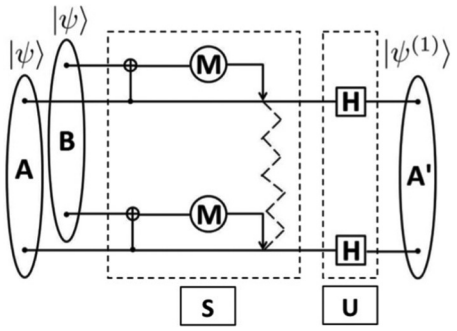


FIG. 1. A schematic diagram (similar to what is used in Ref. [2]) illustrating one iteration of entanglement purification. The components labeled by M denote the measurement performed on the qubit pair from B. The dashed-line connection denotes the conditional selection of the pair of qubits from A based on the outcome of the measurement performed on the qubit pair from B. If both yield 0, the qubit pair from A will be retained. Otherwise, they will be discarded. The qubits that pass the selection are transformed by a pair of Hadamard gates.

the simplicity of our modified purification model (so that the evolving state will stay in the subspace spanned by $|00\rangle$ and $|11\rangle$), the time lapse between **S** and **U** within one iteration step is still ignored.

With the time evolution of the system over the $\Delta t$ period accounted for, the overall map after two successive purification iterations then become

$$\xi \to g(\xi) = \frac{2\xi^2}{1+\xi^4} \exp\left(-\frac{iE\Delta t}{\hbar}\right), \tag{2}$$

where $E$ is the energy difference between states $|11\rangle$ and $|00\rangle$. For convenience we now use the phase factor $\phi \equiv E\Delta t/\hbar$ as a parameter to describe the system's natural time evolution. All possible effects of the system's natural time evolution are now captured by $\phi$ and the map in Eq. (2) is the main subject of our numerical investigation. In cases where the extra phase factor is not of interest, then it can be canceled if a "spin-echo" technique is applied. Specifically, if we place two additional NOT gates in the purification process as shown in Fig. 3, then a simple calculation shows that the nonlinear map described in Eq. (1) can be recovered.

## III. RESULTS FOR FIXED VALUES OF $\phi$

The convergence of the states (i.e., the value of $\xi$ shown on a complex plane after a number of iterations) under the purification map in Eq. (2) is summarized in Fig. 4. First of all, for $\phi = \pi/2$, the convergence pattern coincides with the results obtained by Kiss *et al.* [2].

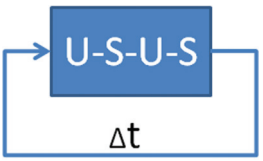


FIG. 2. (Color online) Schematic illustration of a purification step with the system's own time evolution over a time period of $\Delta t$ between every two successive iterations.

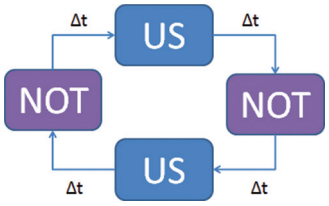


FIG. 3. (Color online) Schematic representation of the modified purification process in which the effects of natural time evolution are cancelled.

This can be understood from the following relation between cases of $\phi = \pi/2$ and $\phi = 0$:

$$[g^{o(n)}(\xi)]_{\phi=\pi/2} = [g^{o(n)}(\xi)]_{\phi=0} e^{-i\frac{\pi}{2}(2^n-1)}, \tag{3}$$

that is, the results of the two maps differ only by a pure phase factor. Second, all the shown patterns have an attractive region in the center, with a radius $\rho \approx 0.543$ where $|g(\xi)|$ asymptotically converges to (0,0). Third, for the region outside radius $\rho = 2$ all values of $\xi$ converge to (0,0).

Fixed points of period $n$ of the map can be found by evaluating $g^{\circ n}(\xi) = \xi$. Specifically, the function $g(\xi)$ acting on $\xi = (x, y)$ can be regarded as a transformation on the complex

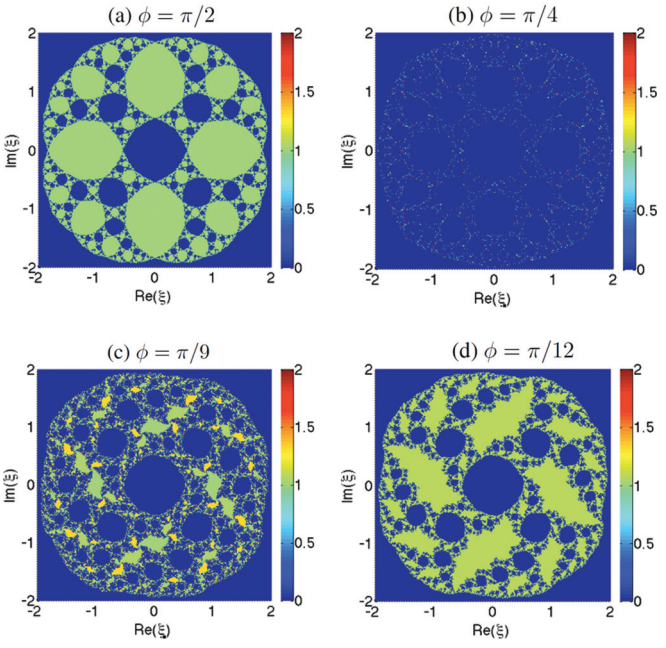


FIG. 4. (Color online) Convergence pattern of initial values of $\xi$ for (a) $\phi = \pi/2$ to two fixed points (0,0) and (0,1) denoted by the color blue and green on the complex plane, respectively, (b) $\phi = \pi/4$ showing most initial values of $\xi$ have converged to (0,0) after 30 iterations, (c) $\phi = \pi/9$ to the fixed point (0,0) and to an attracting cycle of period 3, and (d) $\phi = \pi/12$ to two fixed points (0,0) and (1.05233,0.21486) denoted by the color blue and green, respectively. (a), (c), and (d) Display asymptotic behaviors of the entanglement evolution dynamics. (b) Displays behaviors after only 30 iterations; long-term behavior is such that all initial values of $\xi$ converge to (0,0).

plane,

$$\begin{pmatrix} x \\ y \end{pmatrix} \longrightarrow \begin{pmatrix} \mathrm{Re}\{g(x,y)\} \\ \mathrm{Im}\{g(x,y)\} \end{pmatrix}. \tag{4}$$

The linear stability matrix **M** can be written as the Jacobian matrix for this transformation,

$$\mathbf{M} = \begin{pmatrix} \frac{\partial \mathrm{Re}\{g(x,y)\}}{\partial x} & \frac{\partial \mathrm{Re}\{g(x,y)\}}{\partial y} \\ \frac{\partial \mathrm{Im}\{g(x,y)\}}{\partial x} & \frac{\partial \mathrm{Im}\{g(x,y)\}}{\partial y} \end{pmatrix}. \tag{5}$$

To determine the stability of a particular fixed point, the eigenvalue ($\omega_i$) of the linear stability matrix is evaluated at that fixed point. By looking into the eigenvalues of the stability matrix **M** at the fixed points associated with $\phi = \pi/2$, two stable fixed points were found to be at (0,0), which corresponds to a totally separable state, and (0,1), which corresponds to the maximally entangled state $|\psi\rangle = \frac{1}{\sqrt{2}}(|00\rangle + \mathrm{i}|11\rangle)$.

Next we study cases with $\phi \neq \pi/2$. For $\phi = \pi/12$ [see Fig. 4(d)], the linear stability analysis shows that $|g(\xi)|$ converges to (1.05233,0.21486) instead of (0,1) on the complex plane. The output state is therefore no longer a maximally entangled state because the magnitude of the relative phase is $|\xi| = 1.07404$. For $\phi = \pi/9$ [see Fig. 4(c)], it is observed that the values of $|g(\xi)|$ converge to a stable cycle with period 3 in which none of the values correspond to a maximally entangled state. This is intriguing because the existence of period 3 orbits in a nonlinear system is often connected with the existence of orbits of all possible periods [10]. The most drastic change in the convergence patterns, however, is observed for $\phi = \pi/4$ [Fig. 4(b)]: $|g(\xi)|$ asymptotically approaches (0,0) for all values of $\xi$. Physically, this means that all initial states will converge to a separable state for a purification process with the phase factor $\phi = \pi/4$. The linear stability analysis confirms that (0,0) is indeed the only stable fixed point for this case. This indicates that the system's own time evolution can have a huge influence on the entanglement evolution dynamics.

## IV. BIFURCATION DIAGRAM AND FINITE-TIME EXPONENTIAL SENSITIVITY

In this section we investigate the evolution of a maximally entangled state, with the phase parameters ranging from $\phi = 0$ to $\phi = \pi$. To present the impact of $\phi$ via a bifurcation diagram, we choose the Bell's state $|\Phi^+\rangle = \frac{1}{\sqrt{2}}(|00\rangle + |11\rangle)$ as the initial state. The results are shown in Fig. 5, which depicts the behavior of the evolution emanating from $|\Phi^+\rangle$ for the first 100 iterations of our protocol. As seen from Fig. 5, the bifurcation diagram has a period of $\pi/2$, and it has a strong dependence on $\phi$. In regimes such as $0 < \phi < 0.30$ and $1.30 < \phi < 1.85$, there is very stable convergence with small deviation from a fully entangled state. In addition, there are apparently interesting regimes with very long periods. Echoing with those convergence patterns shown in Fig. 3, the results here once again demonstrate the important role that the natural time evolution of the two qubits can play.

To gain insight into the nature of the attractors associated with each $\phi$, we have also computed the finite-time Lyapunov

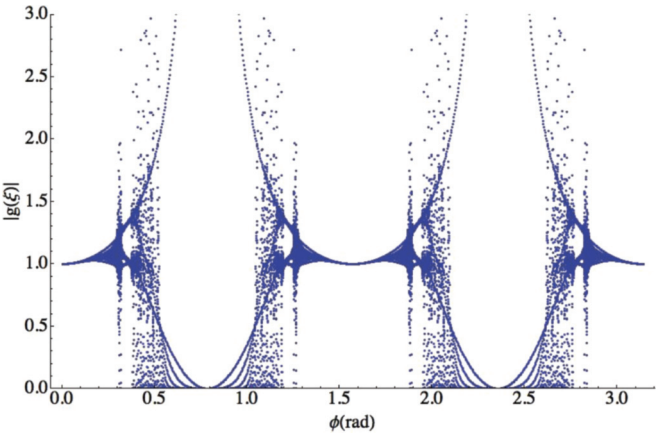


FIG. 5. (Color online) The bifurcation diagram displays the behaviors of $|g(\xi)|$ with fixed initial value of $\xi = (1,0)$ for different values of the phase parameter $\phi$, for the first 100 iterations of Eq. (2).

exponent λ, i.e.,

$$\lambda = \lim_{n\to N} \lim_{\delta d_0 \to 0} \frac{1}{n} \ln \frac{\delta d_n}{\delta d_0}, \tag{6}$$

where $\delta d_k = |g^{\circ k}(\xi_1) - g^{\circ k}(\xi_2)|$ is the separation between two initially slightly different relative phases $\xi_1$ and $\xi_2$ after the $k$th iteration. In our analysis, $N$ is chosen to be a large value but the number of iterations should be before every point is reverted back to 0. The gradient of the least-square fit line on the graph that plots $\ln(\delta d)$ against the number of iterations $n$ is taken to indicate the Lyapunov exponent that corresponds to a particular initial state and phase parameter. Table I shows the Lyapunov exponents for some values of the phase parameter $\phi$ near the chaotic regime with the initial states $\xi_1 = (1,0)$ and $\xi_2 = (1.0001,0.0001)$. The existence of positive (though finite-time) Lyapunov exponents further indicates the exponentially fast separation of two slightly different initial states. The dependence of λ upon $\phi$ also shows that the complexity of the dynamics is strongly correlated with $\phi$.

TABLE I. Finite-time Lyapunov exponents obtained for some values of $\phi$. The exponents corresponding with $\phi = 0.6, 0.7$, and 0.8 are calculated for only the first two iterations because from the third iteration onwards the points start converging to each other when both are attracted to the origin.

| Phase parameter | Lyapunov exponent |
|---|---|
| $\phi$ | λ |
| 0.3 | 0.10 |
| 0.4 | 0.21 |
| 0.425 | 0.44 |
| 0.45 | 0.62 |
| 0.475 | 0.50 |
| 0.5 | 0.44 |
| 0.525 | 0.56 |
| 0.55 | 0.34 |
| 0.6 | 0.17 |
| 0.7 | 4.22 |
| 0.8 | 7.76 |

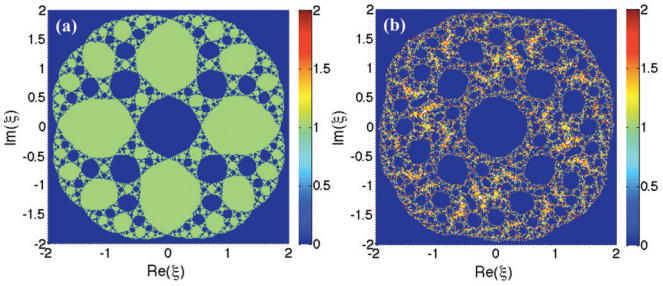


FIG. 6. (Color online) Convergence patterns for a fluctuating phase parameter $\phi$ after 20 iterations. (a) $\phi = \pi/2 \pm 0.10$ and (b) $\phi = \pi/9 \pm 0.10$ (noise fluctuations are uniformly distributed in the indicated intervals). Results here should be compared with those presented in Figs. 4(a) and 4(c).

## V. POSSIBLE APPLICATIONS

### A. Weak or strong sensitivity to $\phi$

For purification-related applications, it should be of interest to examine what values of the phase parameter $\phi$ can make the purification process more resilient to small fluctuations in $\phi$. The bifurcation diagram (Fig. 5) shows that quasimaximally entangled states are preserved by the purification scheme for a wide range of phase parameters around $\phi = \pi/2$. This leads to a possibility of a relatively robust purification scheme after taking into account the system's natural evolution (Strictly speaking, whether a maximally entangled state or an almost maximally entangled state can be preserved also depends on the initial states. However, by referring to the convergence map, one can already roughly know which (initial) states will converge to a maximally entangled state).

We have numerically tested the stability of the convergence patterns by introducing small random fluctuations in the phase parameter $\phi$. That is, after each iteration of the purification protocol, the value of $\phi$ is allowed to fluctuate by a small amount. The results are shown in Fig. 6. For $\phi = \pi/2$, the convergence pattern in Fig. 6(a) with fluctuations $\delta\phi = 0.10$ shows resemblance to the one in Fig. 4(a) with $\phi$ fixed at $\phi = \pi/2$. Any input state in the "green" region in Fig. 6(a) will generate an output state that is maximally entangled. In contrast, for $\phi = \pi/9$ the convergence pattern has changed significantly as compared to Fig. 4(c). For both cases, a too large uncertainty in the phase parameter would destroy the entanglement altogether. We thus conclude that $\phi = m\pi/2$ ($m$ an integer) can be chosen for the sake of a more robust purification process after the system's natural evolution is taken into account.

On the other hand, the strong sensitivity of the purification outcomes to small fluctuations in $\phi$ regimes away from $\phi = \pi/2$ might be useful as well. For example, if the initial state is precisely known and if the error in the operations **S** and **U** are sufficiently small, then this sensitivity may provide a novel tool to detect small phase fluctuations in $\phi$, which may be caused by an environment weakly interacting with the two-qubit system or a weak external field.

### B. Sensitivity to initial states

Finally, we discuss the usefulness of the sensitivity of the purification outcome to the initial states. It was proposed earlier that a strong sensitivity to initial states can be used to distinguish slightly different quantum states exponentially fast [3,11]. For phase parameters with a stable convergence pattern such as $\phi = \pi/2$ [Fig. 4(a)] or $\phi = \pi/12$ [Fig. 4(d)], this scenario would only work if we hope to distinguish states located near the boundaries of different converged states. Interestingly, we may do more than that by exploiting the richer dynamics associated with other values of $\phi$.

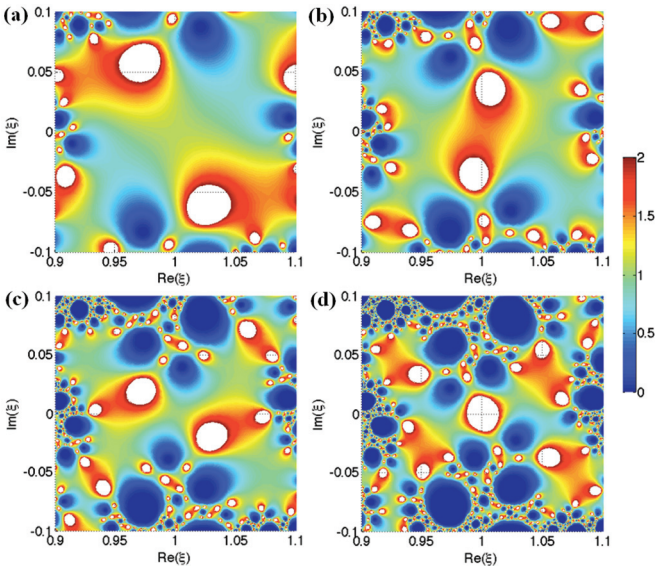


FIG. 7. (Color online) Convergence patterns with $\phi = 1.12$. The number of iteration is 18, 20, 22, and 24 for panels (a)–(d), respectively. The magnitude of the coefficient is indicated by the color bar.

Consider then a convergence pattern shown in Fig. 7, for $\phi = 1.12$. Linear stability analysis shows that (0,0) is the only stable fixed point. After many iterations, the "chaotic" purification dynamics only displays convergence to (0,0), which is similar to the dynamics for $\phi = \pi/4$. However, their explicit evolution histories of the "trajectories" are much different. For a certain finite number of iterations, the convergence pattern shows very fine structure (as shown on the complex plane in the region around the point (1,0) in Fig. 7), whereas the same regime would have all converged to 0 for $\phi = \pi/4$ [Fig. 4(b)].

It seems possible now to make use of the fine structures on the complex plane to facilitate the distinguishing between different initial quantum states. For instance, we can compare an arbitrary state with a state located at the center of one of the white dots in Fig. 7 (corresponding to values of $\xi$ larger than 2). If the given arbitrary state is located outside the area of the white dot, their evolution will be very different (Fig. 7). If the arbitrary state is located within the area of the white dot, both states will converge to the separable state $|\psi\rangle = |00\rangle$. This is simply because all points on the complex plane with $|\xi| > 2$ will be attracted to (0,0) (see Sec. III). The area of the white dot can thus be regarded as a maximum resolution in distinguishing two quantum states. As we consider a larger number of iterations, the area of the white dots decreases and we in principle can have a higher resolution.

There are, however, two major limitations when it comes to experimental realizations. Firstly, since half of the resources

are completely used up in each implementation of the **U**-**S** transformations, to accomplish $n$ iterations we need $2^n$ qubits. The number of qubits required increases rapidly if a large number of iterations is considered. This presents a practical difficulty for implementing this idea. However, this difficulty is perhaps inherent to the purification protocol itself. One solution is to make the purification protocol more efficient by keeping the discarded qubits [9]. Secondly, we have assumed that the phase parameter $\phi$ is not fluctuating. As suggested in the previous subsection, very small randomness in $\phi$ may significantly change the fine structures seen in the convergence pattern. Ultimately, the use of exponential sensitivity as a "Schrödinger's microscope" to distinguish two very close quantum states must account for all the different aspects of a nonlinear quantum map.

## VI. CONCLUSIONS

In this paper, by considering the natural time evolution of a two-qubit system, we have found different types of attractors emerging from the entanglement dynamics associated with a quantum purification protocol. This constitutes a novel example of the interplay between the system's own unitary evolution and some measurement-related nonlinear operations. The nature of the found attractors depends heavily on the phase acquired by the system between two successive purification steps. By investigating the sensitivity of the dynamics to fluctuations in the phase parameter, we have identified a particular parameter regime in which the purification protocol is more stable. We have also discussed the possible use of purification processes in distinguishing between quantum states and in detecting fluctuations in a phase parameter. Our results are hoped to stimulate further studies of quantum nonlinear maps, which are of interest to both areas of nonlinear dynamics and quantum physics.

## ACKNOWLEDGMENT

We thank the Special Program of Science (SPS) at the Faculty of Science, National University of Singapore for making this research work possible.

[1] W. Dür and H. Briegel, Rep. Prog. Phys. **70**, 1381 (2007).
[2] T. Kiss, S. Vymětal, L. D. Tóth, A. Gábris, I. Jex, and G. Alber, Phys. Rev. Lett. **107**, 100501 (2011).
[3] T. Kiss, I. Jex, G. Alber, and S. Vymetal, Phys. Rev. A **74**, 040301 (2006).
[4] T. Kiss, I. Jex, G. Alber, and E. Kollar, Int. J. Quantum. Inform. **6**, 695 (2008).
[5] B. Misra and E. C. G. Sudarshan, J. Math. Phys. (NY) **18**, 756 (1977).
[6] P. Facchi and S. Pascazio, in *Progress in Optics*, edited by E. Wolf, Vol. 42 (Elsevier, Amsterdam, 2001), p. 147.
[7] M. Lewenstein and K. Rzaźewski, Phys. Rev. A **61**, 022105 (2000).
[8] J. B. Gong and S. A. Rice, J. Chem. Phys. **120**, 9984 (2004).
[9] H. Bechmann-Pasquinucci, B. Huttner, and N. Gisin, Phys. Lett. A **242**, 198 (1998).
[10] Edward Ott, *Chaos in Dynamical Systems*, 2nd ed. (Cambridge University Press, Cambridge, 2002).
[11] S. Lloyd and Jean-Jacques E. Slotine, Phys. Rev. A **62**, 012307 (2000).